NEUROSCIENCE

Fast track to the neocortex: A memory engram in the posterior parietal cortex

S. Brodt[1,2]*, S. Gais[1], J. Beck[1], M. Erb[2,3], K. Scheffler[2,3], M. Schönauer[1,2,4]

Models of systems memory consolidation postulate a fast-learning hippocampal store and a slowly developing, stable neocortical store. Accordingly, early neocortical contributions to memory are deemed to reflect a hippocampus-driven online reinstatement of encoding activity. In contrast, we found that learning rapidly engenders an enduring memory engram in the human posterior parietal cortex. We assessed microstructural plasticity via diffusion-weighted magnetic resonance imaging as well as functional brain activity in an object–location learning task. We detected neocortical plasticity as early as 1 hour after learning and found that it was learning specific, enabled correct recall, and overlapped with memory-related functional activity. These microstructural changes persisted over 12 hours. Our results suggest that new traces can be rapidly encoded into the parietal cortex, challenging views of a slow-learning neocortex.

Systems memory consolidation is considered a slow process of neuronal reorganization. Fresh memories rely on the hippocampus, which reinstates the cortical ensembles that were active during encoding, whereas neocortical memory develops more slowly, through frequent reactivation (*1*, *2*). Recent findings suggest that the posterior parietal cortex (PPC) can acquire a memory representation rapidly during learning (*3*, *4*). It is unclear whether these early contributions go beyond an online reinstatement of previous activity or whether they originate from a true neocortical engram. Methodological advances have made it possible to track engrams in rodents, yet they have remained elusive in humans (*5*–*7*). In humans, multivariate analysis of functional magnetic resonance imaging (fMRI) can assess active memory representations during encoding and retrieval (*8*, *9*), but this method is unable to distinguish between activity originating within a region and activity reinstated through input from another region. It thus cannot unequivocally reveal the permanent location of the dormant trace.

A memory engram has four defining features: (i) it must relate to a specific experience; (ii) it must engender an enduring change in the neural substrate; (iii) it can lie dormant for extended periods; and (iv) it must enable memory recall, thus having an impact on behavior (*10*, *11*). To elucidate where memory formation leads to lasting physical changes, the microstructural modifications, e.g., of synapse number and morphology, which can occur within minutes after learning must be assessed (*12*). Diffusion-weighted MRI (DW-MRI) is sensitive to the microstructure of brain tissue (*13*) and can image experience-driven structural plasticity in the human brain noninvasively and in vivo (*14*–*16*).

We used fMRI and DW-MRI to demonstrate the dynamic contributions of neocortical areas

[1]Institute of Medical Psychology and Behavioral Neurobiology, University of Tübingen, Tübingen, Germany. [2]Max-Planck-Institute for Biological Cybernetics, Tübingen, Germany. [3]Biomedical Magnetic Resonance, Universitätsklinikum Tübingen, Tübingen, Germany. [4]Princeton Neuroscience Institute, Princeton University, Princeton, NJ, USA.
*Corresponding author. Email: svenja.brodt@uni-tuebingen.de

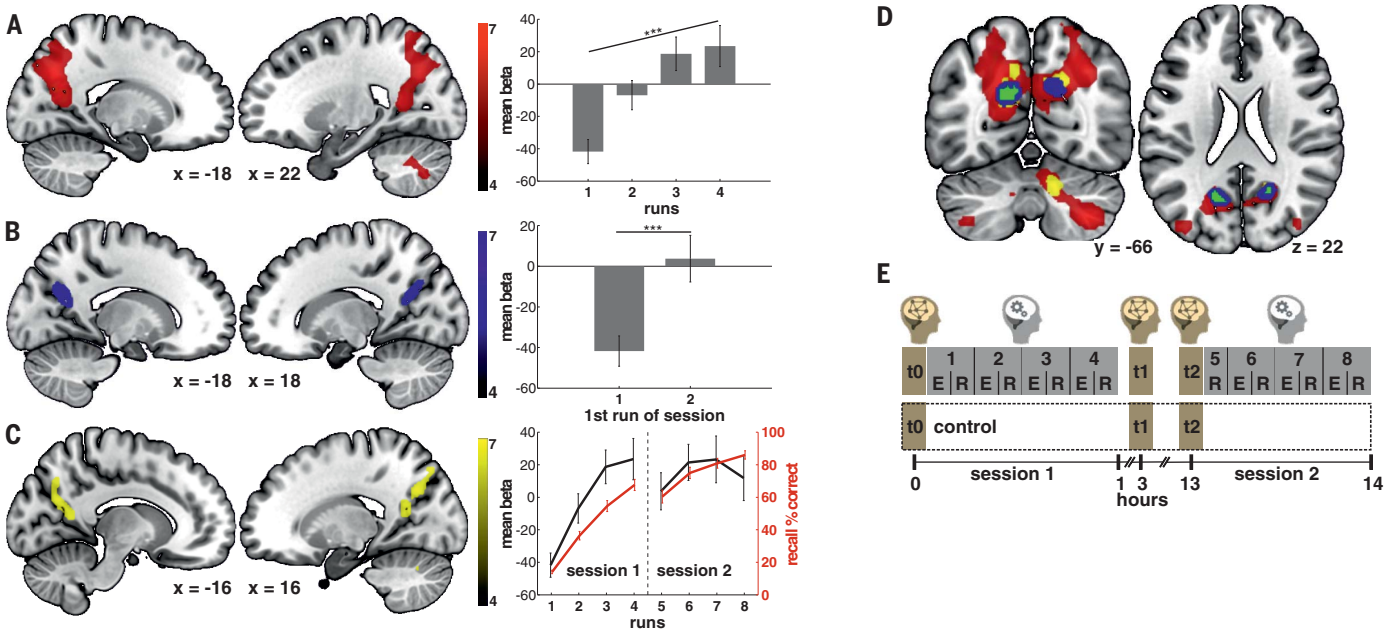

Fig. 1. Experience dependence, persistence, and correlation with performance of PPC activity during memory recall. (**A**) Experience-dependent increase with repetition. Mean beta values in the anatomically defined precuneus ROI for the first task session; linear contrast, ***$P < 0.001$, $n = 39$. (**B**) Persistently elevated precuneus responses after 12 hours. Mean beta values; two-sided t test, ***$P < 0.001$, $n = 39$. (**C**) Correlation of precuneus activation with memory performance. Mean beta values, black; mean percentage of correctly recalled item locations, red; one sample t test of z-transformed single-subject correlations, $P < 0.001$, $n = 39$. (**D**) Conjunction of the minimum statistic of all three analyses, green. Clusters exhibited significant peak-level effects at full-volume–corrected $P_{FWE} < 0.05$ and exceeded 10 voxels. No masking. Beta values were corrected for baseline activation. Data are means ± SEM. Corresponding data from encoding are shown in fig. S1 and table S2. (**E**) Experimental design. An object–location learning task was trained for eight encoding (E)–recall (R) runs with fMRI. DW-MRI was measured at t0 to t2. For the control condition, the learning task was omitted.

to memory during two sessions of four encoding–recall repetitions of an object–location association task (Fig. 1E, movie S1, and materials and methods) and to identify the location of the engram engendered by the memory. First, we examined in whole-brain analyses which regions displayed changes in functional activity that indicated memory representations. We identified an experience-dependent, increasing response over repeated retrieval in the bilateral precuneus and areas along the dorsal visual stream, the cerebellum, thalamus, and motor areas (linear increase in the anatomically defined precuneus over first session: $F_{1,38}$ = 26.76, P < 0.001, η^2 = 0.404) (Fig. 1A and table S1A). This increased response to successfully encoded stimuli persisted over a 12-hour offline interval in the precuneus (t_{38} = 4.50, P < 0.001) (Fig. 1B and table S1B). The posterior parietal areas were also the only regions for which there was a significant correlation between memory performance and functional brain activity over retrieval repetitions (average correlation on the single-subject level: r = 0.378, t_{38} = 6.15, P < 0.001) (Fig. 1C and table S1C). The above contrasts did not yield significant clusters in an anatomical region of interest (ROI) analysis of the hippocampus; however, we

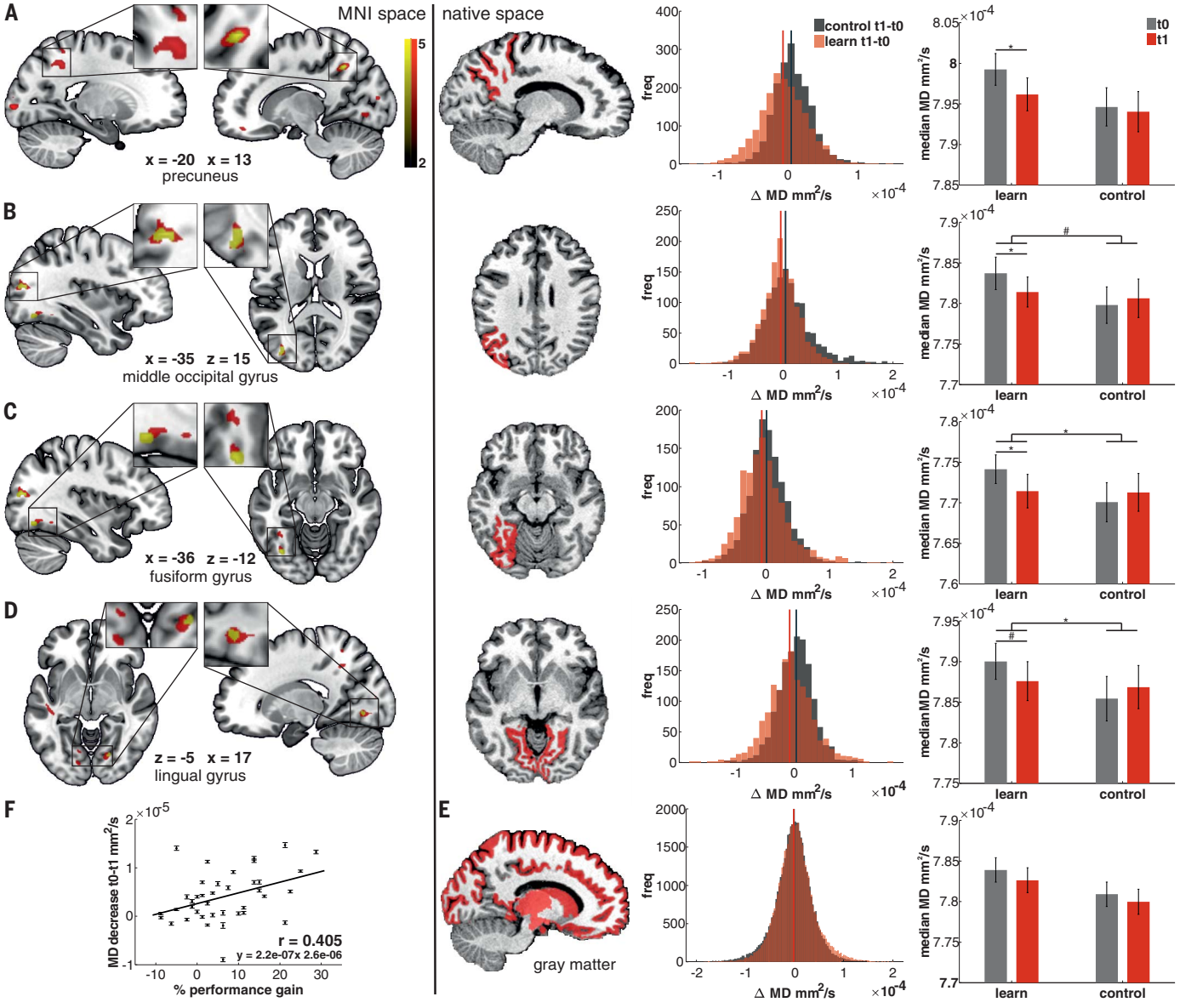

Fig. 2. Learning induces rapid microstructural changes in the neocortex. Statistical maps on the left display whole-brain Montreal Neurological Institute (MNI) space group-level analyses. Significant decrease from t0 to t1 for the learning condition, red, n = 39; significant interaction with the control condition, yellow, n = 33. Two-sided t tests. Clusters exhibited significant peak-level effects at P_{uncorr} < 0.001 and exceeded 10 voxels. No masking. ROI analysis on the anatomically defined precuneus confirmed peak-level effects at P_{FDR} < 0.05. The middle column shows sample gray matter masks of the native space analyses on the raw, unsmoothed MD of the anatomically defined gray matter ROIs. Distribution plots on the right show sample subject distributions of MD differences between t0 and t1 for all ROI voxels. Learning condition, red; control condition, gray; vertical lines represent medians. All ROIs in (**A**) to (**D**), but not the remaining gray matter (**E**), showed a left shift of the learning distribution, indicating an MD decrease and thus learning-induced structural plasticity. Bar graphs on the far right show group-level analyses, which confirmed region-specific learning-induced MD decreases. Repeated-measures ANOVAs, n = 33. #P < 0.07, *P < 0.05. Data are means ± SEM. (**F**) The mean raw MD decreases from t0 to t1 of all four ROIs were highly correlated to the overall performance improvement from session 1 to session 2. Pearson correlation, n = 39. Dots are single-subject values, and error bars are SEM.

observed a subsequent memory effect during encoding runs in the first task session, consistent with a role of the hippocampus in early encoding (fig. S4, table S9, and supplementary text). In contrast, a strict conjunction analysis confirmed that only the precuneus simultaneously fulfilled all of the above criteria (Fig. 1D and table S1D). Finally, to assess whether the activity patterns in the precuneus were content specific, we performed a multivariate pattern analysis. This analysis showed that it is possible to decode category information of the stimuli from this area during memory encoding ($P < 0.001$) (fig. S2 and table S3). Our findings showed that the precuneus can hold a representation of retrieved information (*8*, *17*–*20*). Still, the question remains, what type of information is processed in this area. We used associative, explicitly learned material, which is, because of the low number of learning repetitions, at the border between episodic and semantic memory. The precuneus is tightly integrated into a network of memory-related brain regions (*21*) and is located at the crossroads of multiple sensory pathways, which makes it ideal for the processing of abstract information or higher-order multimodal associations and a likely convergence zone for distributed memory functions. In fact, the parietal cortex plays a critical role in integrating new information into existing schemas and has been identified as a major node in the semantic system (*22*, *23*).

To qualify as an engram, a memory representation must induce persistent structural plasticity. DW-MRI, and in particular mean diffusivity (MD), allows measurement of changes in brain microstructure. Though it is only an indirect measure, there is strong evidence that decreased MD can reflect mechanisms of learning-dependent plasticity, e.g., astrocyte, myelin, or synaptic remodeling. Synapse density, brain-derived neurotrophic factor expression, and astrocyte activation increase after learning at the sites where MD decreases, suggesting a tight link to experience-induced structural plasticity (*14*, *16*, *24*). Traditional views suggest that learning-related changes in the neocortex need frequent hippocampal reactivation over extended periods to develop (*2*). Unexpectedly, we found robust microstructural changes, reflected by decreases in MD, already at 90 min after learning in several bilateral areas along the dorsal and ventral visual streams (Fig. 2, left, and table S4A), particularly in the precuneus [false discovery rate–corrected P value (P_{FDR}) < 0.05], but not in the hippocampus (see the supplementary text). To test whether these changes were learning specific, we compared them with changes observed in a control condition without learning between scans. We found significant learning-induced changes in the left precuneus (Fig. 2A and table S4B), the left middle occipital gyrus (Fig. 2B), the left fusiform gyrus (Fig. 2C), and the bilateral lingual gyri (Fig. 2D). For these four regions, analyses of variance (ANOVAs) on the mean raw MD values confirmed that the significant interaction effect was based on MD decreases in the learning condition and not in the control condition (table S5A). Analyses of the raw, unsmoothed, subject-native space MD data further corroborated these findings (Fig. 2, right, and table S5B). These morphological changes also correlated with memory performance. Subjects with higher structural plasticity had better memory retention from session 1 to session 2 (r_{39} = 0.405, P = 0.010) (Fig. 2F).

The final criterion of a memory engram is that it persists over time. We measured long-term MD changes 12 hours after learning. All regions that showed rapid learning-induced structural plasticity maintained these changes for more than 12 hours. A significant long-lasting reduction in MD was found again bilaterally in the precuneus, along the dorsal and ventral visual processing streams, and in frontal regions [uncorrected P value (P_{uncorr}) < 0.001] (Fig. 3 and table S6A). These changes did not occur in the control condition (interaction with control: P_{uncorr} < 0.005) (Fig. 3 and table S6B). Analyses of the mean raw MD values again confirmed this finding (Fig. 3, right, and table S5C). Using a whole-brain joint inference approach, we further identified the precuneus, the middle occipital gyrus, and the lingual gyrus as regions in which rapid and persistent learning-dependent structural plasticity can be found (Fig. 3E and table S7). Previous studies have mostly measured rapid structural plasticity in the human brain at delays similar to our short interval. Our data show that the microstructural changes in the regions that display learning-induced rapid structural plasticity remain stable for at least 12 hours.

We identified posterior parietal areas that fulfilled all defining conditions of a memory engram, i.e., they showed functional responses that were specifically related to the memory, were persistent over longer offline periods, and were relevant for later memory recall. These

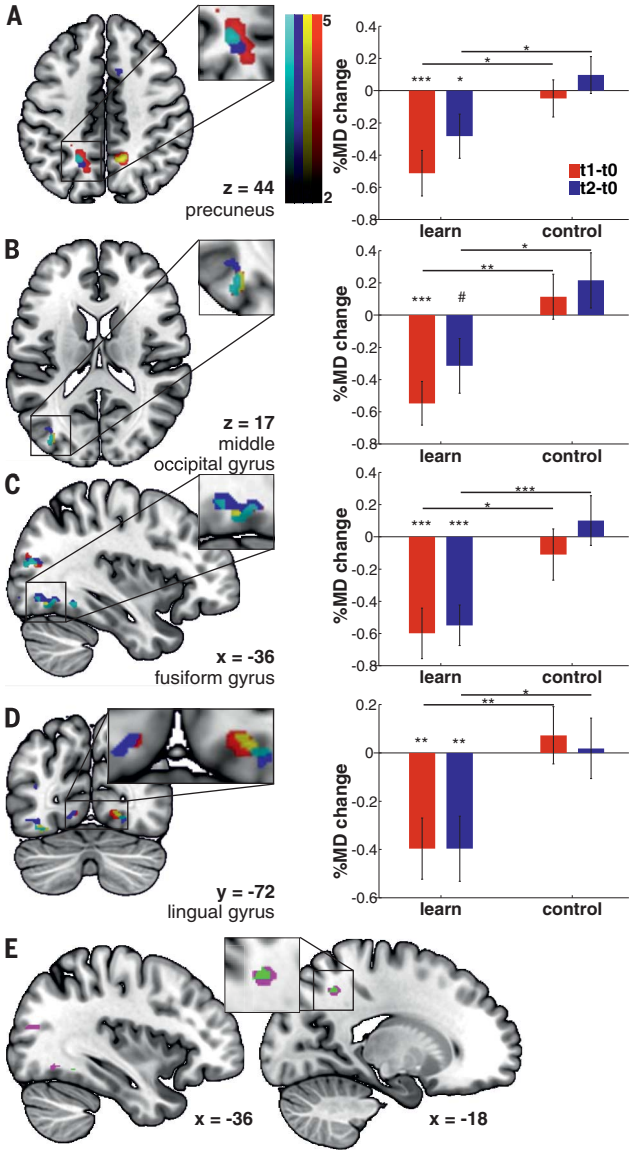

Fig. 3. Learning-induced persistent microstructural changes in the neocortex. (**A** to **D**) Long-term MD decreases. (Left) Whole-brain MNI space group-level analyses. Decreases from t0 to t2 for the learning condition, blue, n = 39; interaction with the control condition, cyan, n = 33. Short-term changes from Fig. 2 are shown in red and yellow. Two-sided t tests. All clusters exhibited significant peak-level effects at P_{uncorr} < 0.001 (learning condition) and P_{uncorr} < 0.005 (interaction) and exceeded 10 voxels. No masking. (Right) Mean raw MD changes for short-term (red) and long-term (blue) intervals. Repeated-measures ANOVAs confirmed that the interaction effects stem from a selective decrease in the learning condition. #$P \leq 0.07$, *$P < 0.05$, **$P < 0.01$, ***$P \leq 0.001$, n = 33. Data are means ± SEM. (**E**) Joint inference analyses on short-term and long-term MD decreases. Nonparametric combination test, purple, n = 33; conjunction analysis of the minimum statistic, green, P_{uncorr} < 0.001, n = 39. Clusters exceeded 10 voxels. No masking.

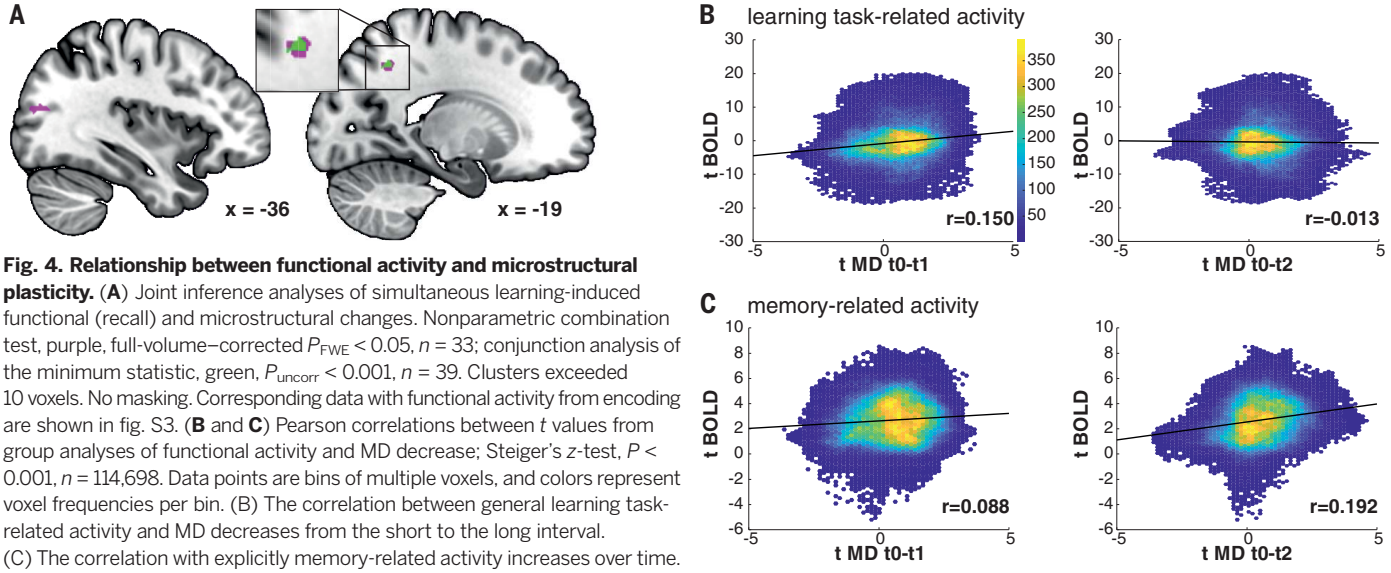

Fig. 4. Relationship between functional activity and microstructural plasticity. (**A**) Joint inference analyses of simultaneous learning-induced functional (recall) and microstructural changes. Nonparametric combination test, purple, full-volume–corrected $P_{FWE} < 0.05$, $n = 33$; conjunction analysis of the minimum statistic, green, $P_{uncorr} < 0.001$, $n = 39$. Clusters exceeded 10 voxels. No masking. Corresponding data with functional activity from encoding are shown in fig. S3. (**B** and **C**) Pearson correlations between t values from group analyses of functional activity and MD decrease; Steiger's z-test, $P < 0.001$, $n = 114{,}698$. Data points are bins of multiple voxels, and colors represent voxel frequencies per bin. (B) The correlation between general learning task-related activity and MD decreases from the short to the long interval. (C) The correlation with explicitly memory-related activity increases over time.

regions also showed structural–plastic changes that conformed to the same criteria. Thus, a true neocortical engram developed rapidly, after only four rounds of rehearsal. Similarly, studies in rodents have revealed that neocortical engram cells are already tagged during encoding and have detected experience-dependent microstructural changes as early as 1 hour after learning (*5*, *6*, *25*, *26*). We suggest that such rapid learning-induced neocortical plasticity arises from multiple encoding–recall repetitions (*4*, *27*). The PPC's ability to accumulate new information over several minutes (*28*) and learn associations between well-known object schemata (*29*) might allow particularly fast neocortical memory formation.

We next used joint inference to identify regions that meet mnemonic criteria in both imaging modalities. A nonparametric combination approach yielded significant clusters in the middle occipital gyrus [family-wise error corrected P value (P_{FWE}) < 0.05] (Fig. 4A and table S8A) and the precuneus. The latter also survived a strict conjunction analysis ($P_{uncorr} < 0.001$) (Fig. 4A and table S8B). Thus, diffusivity decreased in regions that were functionally involved in memory. Observed online memory representations are thus likely to rely on a true neocortical engram. Looking more broadly at the brain-wide relation between functional activity and structural plasticity, we found that learning task-related functional activity was associated with short-term decreases in MD (correlations of group-level t values, n = 114,698 voxels; short term: $r = 0.150$, long term: $r = -0.013$; difference: $z = 67.09$, $P < 0.001$) (Fig. 4B), whereas the memory-related linear increase in functional activity correlated more strongly with the long-term MD decrease (short term: r = 0.088; long term: $r = 0.192$; difference: $z = -42.98$, $P < 0.001$) (Fig. 4C). These findings suggest that different processes might underlie the microstructural changes at different time points after learning.

Although there is still debate about the functions of the different subregions of the PPC and their roles in working memory, memory-related attention, or reinstatement of previous experience (*3*, *8*), our study highlights the role of the medial PPC. Observing microstructural changes in the precuneus takes us from memory processing and reinstatement to the memory engram itself (*17*). The fast temporal dynamics that we observed challenge traditional models of slow systems consolidation (*2*) and suggest that new traces are encoded rapidly in the neocortex from the onset of learning. In addition, we detected learning-specific, persistent microstructural changes upstream along the dorsal and ventral visual pathways, which is in line with the notion of distributed neocortical memory traces (*8*, *11*). Apart from their role in perception, visual areas process memory content, suggesting memory storage also at this level (*30*, *31*). Indeed, many accounts regard perception and memory not as faculties of different systems but as being localized within the same distributed neural circuits (*28*). Combining functional imaging with diffusion imaging might help transform our view of how the brain translates perception into memory.

REFERENCES AND NOTES

1. J. L. McGaugh, *Science* **287**, 248–251 (2000).
2. P. W. Frankland, B. Bontempi, *Nat. Rev. Neurosci.* **6**, 119–130 (2005).
3. C. Sestieri, G. L. Shulman, M. Corbetta, *Nat. Rev. Neurosci.* **18**, 183–192 (2017).
4. S. Brodt *et al.*, *Proc. Natl. Acad. Sci. U.S.A.* **113**, 13251–13256 (2016).
5. T. Kitamura *et al.*, *Science* **356**, 73–78 (2017).
6. E. Lesburguères *et al.*, *Science* **331**, 924–928 (2011).
7. S. Tonegawa, X. Liu, S. Ramirez, R. Redondo, *Neuron* **87**, 918–931 (2015).
8. B. A. Kuhl, J. Rissman, M. M. Chun, A. D. Wagner, *Proc. Natl. Acad. Sci. U.S.A.* **108**, 5903–5908 (2011).
9. T. I. Brown *et al.*, *Science* **352**, 1323–1326 (2016).
10. R. Semon, *Mnemic Psychology* (G. Allen & Unwin Limited, 1923).
11. S. A. Josselyn, S. Köhler, P. W. Frankland, *Nat. Rev. Neurosci.* **16**, 521–534 (2015).
12. E. R. Kandel, *Science* **294**, 1030–1038 (2001).
13. S. Mori, J. Zhang, *Neuron* **51**, 527–539 (2006).
14. Y. Sagi *et al.*, *Neuron* **73**, 1195–1203 (2012).
15. S. Hofstetter, N. Friedmann, Y. Assaf, *Brain Struct. Funct.* **222**, 1231–1241 (2017).
16. T. Blumenfeld-Katzir, O. Pasternak, M. Dagan, Y. Assaf, *PLOS ONE* **6**, e20678 (2011).
17. J. Chen *et al.*, *Nat. Neurosci.* **20**, 115–125 (2017).
18. A. Gonzalez *et al.*, *Proc. Natl. Acad. Sci. U.S.A.* **112**, 11066–11071 (2015).
19. U. Rutishauser, T. Aflalo, E. R. Rosario, N. Pouratian, R. A. Andersen, *Neuron* **97**, 209–220.e3 (2018).
20. A. Akrami, C. D. Kopec, M. E. Diamond, C. D. Brody, *Nature* **554**, 368–372 (2018).
21. R. L. Buckner, J. R. Andrews-Hanna, D. L. Schacter, *Ann. N. Y. Acad. Sci.* **1124**, 1–38 (2008).
22. A. Gilboa, H. Marlatte, *Trends Cogn. Sci.* **21**, 618–631 (2017).
23. J. R. Binder, R. H. Desai, *Trends Cogn. Sci.* **15**, 527–536 (2011).
24. R. J. Zatorre, R. D. Fields, H. Johansen-Berg, *Nat. Neurosci.* **15**, 528–536 (2012).
25. T. Xu *et al.*, *Nature* **462**, 915–919 (2009).
26. K. K. Cowansage *et al.*, *Neuron* **84**, 432–441 (2014).
27. J. W. Antony, C. S. Ferreira, K. A. Norman, M. Wimber, *Trends Cogn. Sci.* **21**, 573–576 (2017).
28. U. Hasson, J. Chen, C. J. Honey, *Trends Cogn. Sci.* **19**, 304–313 (2015).
29. D. Tse *et al.*, *Science* **316**, 76–82 (2007).
30. S. A. Harrison, F. Tong, *Nature* **458**, 632–635 (2009).
31. J. P. Gavornik, M. F. Bear, *Nat. Neurosci.* **17**, 732–737 (2014).

ACKNOWLEDGMENTS

Funding: This project was supported by the European Social Fund and by the Ministry of Science, Research and the Arts Baden-Württemberg. **Author contributions:** S.B., S.G., M.E., K.S., and M.S. designed the research; S.B., J.B., M.E., and M.S. performed the experiments; S.B. and J.B. analyzed the functional and behavioral data; S.B. analyzed the diffusion data; S.B., S.G., and M.S. wrote the manuscript. **Competing interests:** The authors declare no competing interests. **Data and materials availability:** The raw data and computer code necessary to understand and assess the conclusions of the study can be downloaded from the Open Science Framework platform: osf.io/pnxje.

SUPPLEMENTARY MATERIALS

www.sciencemag.org/content/362/6418/1045/suppl/DC1
Materials and Methods
Supplementary Text
Figs. S1 to S4
Tables S1 to S9
References (*32*–*51*)
Movie S1

22 May 2018; accepted 10 October 2018
10.1126/science.aau2528

Fast track to the neocortex: A memory engram in the posterior parietal cortex

S. Brodt, S. Gais, J. Beck, M. Erb, K. Scheffler and M. Schönauer

Science **362** (6418), 1045-1048.
DOI: 10.1126/science.aau2528

Memories reach the cortex rapidly

How fast do learning-induced anatomical changes occur in the brain? The traditional view postulates that neocortical memory representations reflect reinstatement processes initiated by the hippocampus and that a genuine physical trace develops only through reactivation over extended periods. Brodt *et al.* combined functional magnetic resonance imaging (MRI) with diffusion-weighted MRI during an associative declarative learning task to examine experience-dependent structural brain plasticity in human subjects (see the Perspective by Assaf). This plasticity was rapidly induced after learning, persisted for more than 12 hours, drove behavior, and was localized in areas displaying memory-related functional brain activity. These plastic changes in the posterior parietal cortex, and their fast temporal dynamics, challenge traditional views of systems memory consolidation.

Science, this issue p. 1045; see also p. 994